

Fully Three-dimensional Simulation and Modeling of a Dense Plasma Focus

B. T. Meehan, J. H. J. Niederhaus

Abstract—A Dense Plasma Focus (DPF) is a pulsed-power machine that electromagnetically accelerates and cylindrically compresses a shocked plasma in a Z-pinch. The pinch results in a brief (~ 100 nanosecond) pulse of X-rays, and, for some working gases, also a pulse of neutrons. A great deal of experimental research has been done into the physics of DPF reactions, and there exist mathematical models describing its behavior during the different time phases of the reaction. Two of the phases, known as the inverse pinch and the rundown, are approximately governed by magnetohydrodynamics, and there are a number of well-established codes for simulating these phases in two dimensions or in three dimensions under the assumption of axial symmetry. There has been little success, however, in developing fully three-dimensional simulations. In this work we present three-dimensional simulations of DPF reactions and demonstrate that 3D simulations predict qualitatively and quantitatively different behavior than their 2D counterparts. One of the most important quantities to predict is the time duration between the formation of the gas shock and Z-pinch, and the 3D simulations more faithfully represent experimental results for this time duration and are essential for accurate prediction of future experiments.

Index Terms—Dense Plasma Focus, Magnetohydrodynamics, Simulation and Modeling, Controlled Fusion

I. INTRODUCTION

THERE is an extensive literature on experiments performed with Dense Plasma Focus (DPF) machines, exploring both fundamental Z-pinch physics [1], [2], [3] and applications of the DPF to fields like X-ray lithography [4], fusion energy [5], and modeling of astrophysics [6], to name a few. The vast majority of research has been driven by theory and experimentation, but there is a shift towards developing new experiments informed by computational models and simulations. Many of the simulations that have been used to design DPF experiments are 1-dimensional, in the sense that current, temperature, or expected neutron yield are computed as a function of a single parameter being varied [7]. There has also been work to develop codes that are capable of full magnetohydrodynamic (MHD) modeling of the inverse pinch and run-down phases of the DPF reaction on spatial domains (see Section II for descriptions of the reaction phases), and there exist 2D simulations modeling the physics of the DPF, which are often extended to 3D assuming axial symmetry [8]. Despite some success with 1D and 2D simulations, fully 3D simulations of the MHD phases of the DPF – which do not impose symmetry on the physics of the reaction – are difficult,

and the literature presenting the results of such simulations is sparse. There are a number of challenges in the 3D modeling, including the computational complexity of the problem, a need for appropriate initial conditions to ignite the inverse pinch, insufficient equation of state (EOS) data for the working gas and the electrodes, and incorporating radiative effects into the MHD model.

In a DPF, a working gas is charged, forming a plasma, that travels down an anode surrounded by a cathode, and the speed that the plasma shock travels down the anode is determined by the initial pressure and voltage in the system. The Z-pinch occurs when the plasma shock gets to the end of the anode. The energy available to the Z-pinch is maximized when the current through the DPF is maximized, which means that the rundown time is one of the most important quantities to properly simulate. If simulations correctly predict rundown for a given initial pressure and voltage configuration, those settings can be used in actual experimentation ensuring that the Z-pinch occurs with maximum energy, which in turn results in maximum neutron yield. The neutron yield can be determined experimentally using a Beryllium activation detector [9] (for deuterium fusion), or a Praseodymium activation detector [10] (for deuterium-tritium fusion). Further, when deuterium, or deuterium-tritium mixtures are used as a fill gas, the neutron yield has a power-law relationship [11] with the maximum current, which means that it is also important to be able to faithfully simulate the maximum current. For these reasons, most of our analysis centers on comparing experimentally-measured current waveforms to the simulated current waveform.

In this work, we present simulation results of a fully 3D MHD model of a DPF using the ALEGRA [12] multiphysics code developed at Sandia National Laboratories. The simulations are run in both 2D and 3D, and the results are compared to each other as well as to experiments run in the DPF lab at National Security Technologies, LLC. The predictions of the 2D and 3D computations are qualitatively and quantitatively different, as the 2D simulations show systematically lower inductance, which results in systematically higher currents but unrealistically fast rundown times. The 3D simulations predict lower maximum current values but accurately represent the true rundown time shown in experimental data. This demonstrates that, despite the symmetric geometry of the machine, there are three-dimensional effects present in the MHD physics that must be accounted for in order to faithfully predict the outcome of DPF experiments.

B. T. Meehan is with National Security Technologies, LLC, a Department of Energy Contractor, e-mail: meehanbt@nv.doe.gov

J. H. J. Niederhaus is a Computer Scientist at Sandia National Laboratories, email: jhniede@sandia.gov

Manuscript received December 1, 2012; revised January 11, 2013.

II. DPF PHYSICS AND THE EXPERIMENTAL SETUP

The DPF used in our experiments, and the geometry of which was modeled in the simulations, is formed of coaxial electrodes in a rarified deuterium atmosphere (about 7 Torr). A two-stage Marx capacitor bank is charged, and when discharged, breaks down the gas, forming a shock and starting the “inverse pinch” phase of the reaction, in which the gas expands outward from the anode to the cathode bars (see Fig. 1). Once the gas touches the cathode, the “run-down” phase begins, and the plasma moves up the anode until it Z-pinches at the top of the anode. These two phases, the inverse pinch and rundown, are approximately governed by magnetohydrodynamics and are the components of the reaction that are studied and simulated.

A. DPF Geometry and Setup

Fig. 1 shows the DPF setup used in our experiments. The outer electrode (cathode) is formed of 24 copper bars, 0.375 inches thick and 30.75 inches tall, in a ring with an inside diameter of 6 inches. The cathode is at ground potential, and its bars are shorted at the top with a ring of copper. The anode is a hollow copper tube with an outer diameter of 4 inches that stands 23.6 inches above the ground plane, capped with a hemisphere. The vacuum chamber is 1 foot in diameter, and roughly 6 inches taller than the cathode cage. A Pyrex insulator tube, which is about 0.5 inches thick and stands 8.63 inches above the cathode base, separates the anode and cathode.

The DPF is driven by a two-stage Marx capacitor bank, which is connected to the plasma focus tube by 36 coaxial cables. The total capacitance of the bank (when configured for discharge) is 432 μF , and the maximum total voltage in discharge configuration is 70 kV, which makes the maximum stored energy of the bank 1 MJ. The plasma shock is driven by an external circuit, and the circuit model used in the MHD simulations is shown in Fig. 2. The discharge switch in the circuit represents a collection of eight rail-gap switches that are simultaneously triggered by a single spark gap. The series inductance represents the transmission lines that feed power to the plasma focus tube and was determined empirically by fitting exponentially-dampened sine waves to the experimental data. The 10 nF capacitor in series with the small resistor represents the imperfect capacitance of the terminal plates and the transmission lines that supply the power to the plasma focus tube. The 120 Ω resistor in parallel with the plasma focus tube is the equivalent parallel resistance of the safety resistors.

B. Faraday Current Diagnostic

The discharge current diagnostic is important for comparing simulations to experiment, because it allows for the measurement of both the maximum current through and rundown time of the DPF. As was noted above, these are two of the most important quantities for simulations in order to accurately predict neutron yield and to ensure that the maximum current runs through the system at the time of the Z-pinch. On the NSTec DPF, the discharge current is measured with a

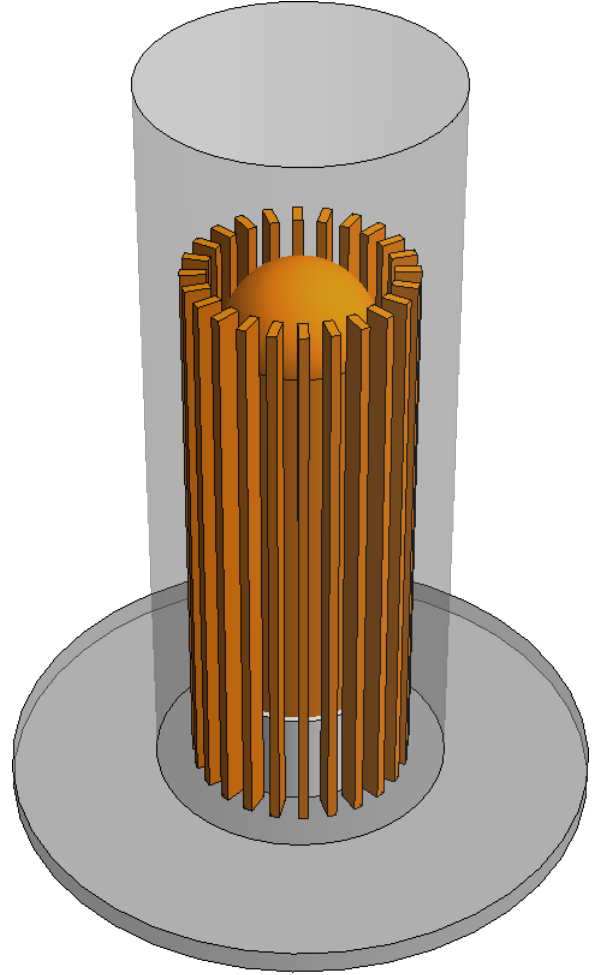


Fig. 1. A rendering of the DPF used for the models and experiments. The anode is the dome-topped cylinder in the center; the cathode “cage” is the collection of rectangular bars that surrounds the anode; and the insulator is visible through the bars, at the bottom of the cathode cage. The vacuum envelope is represented as the tall cylinder that surrounds the cathode and anode, and the ground plate is the flat cylinder at the bottom. Some support features, such as the cathode top support ring, have been left out of the drawing.

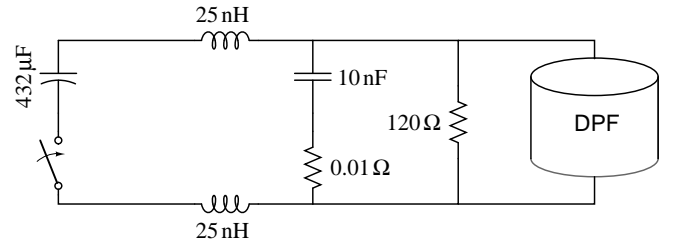


Fig. 2. The equivalent DPF discharge circuit used in the MHD models. The top connection of the DPF is to the anode, and the bottom connection is to the cathode. The switch shown is a collection of eight triggered rail-gap switches.

Faraday rotator [13], which uses the magnetically-induced linear polarization rotation in quartz fibers to measure the current in a circuit. The fiber is wound in a circular fashion around the anode, an orientation that causes the fiber to follow the direction of the magnetic field, allowing it to accurately measure the current. In (1), the polarization rotation angle,

Θ (in radians), is related to the permeability of the vacuum, μ_0 , the current, I , the Verdet constant of the fiber, V , and the number of loops the fiber makes around the anode n . The interaction of the magnetic field, \vec{B} , with an element of the fiber's length, $d\vec{\ell}$, is then integrated over the path of the fiber around the anode. In our arrangement, the fiber wraps around the anode $n = 5.25$ turns. This path is denoted by ξ , and since the fiber is either parallel with the magnetic field or perpendicular to it, the rotation angle is

$$\Theta = V \int_{\xi} \vec{B} \cdot d\vec{\ell} = \mu_0 n V I, \quad (1)$$

in MKSA units. The Faraday rotator current diagnostic is preferred over other discharge current measurements, such as the Rogowski coil, because the Faraday rotator gives current measurements that are not dependent on calibration factors, but rather on an easily measurable geometric quantity: the number of turns around the current to be measured. The only other factor that must be determined is the Verdet constant for the fiber, which can either be measured or obtained from a datasheet on the fiber. When properly set up, the Faraday rotator is a reliable diagnostic.

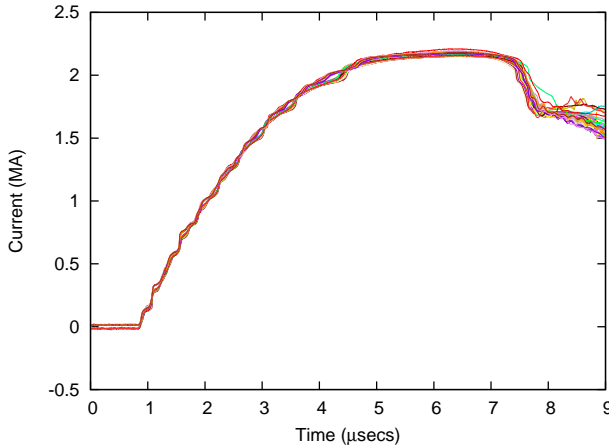


Fig. 3. Shown is a comparison of the current profiles for thirty-seven DPF shots, all at the same voltage and pressure (37.5 kV and 7.28 Torr, respectively). This demonstrates the consistency of the current produced by the machine, as well as representative Faraday rotator data.

Fig. 3 shows experimentally-measured results from the Faraday rotator detector for 37 DPF shots initiated with the same voltage and pressure. As can be seen, the profiles are all nearly identical, which demonstrates both the shot-to-shot consistency of the DPF and the reliability of the Faraday diagnostic. The placement of the Faraday loop is important for understanding the current that it measures. This is easier to show than it is to describe, so this is included as fig. 4.

III. MODELING AND SIMULATION OF THE DPF

The modeling for this project was performed with Sandia National Laboratories' ALEGRA-MHD code. ALEGRA is a finite-element, multi-material, arbitrary Lagrangian-Eulerian (ALE) shock hydrodynamic code designed for parallel computing. It uses an operator-split edge-element formulation

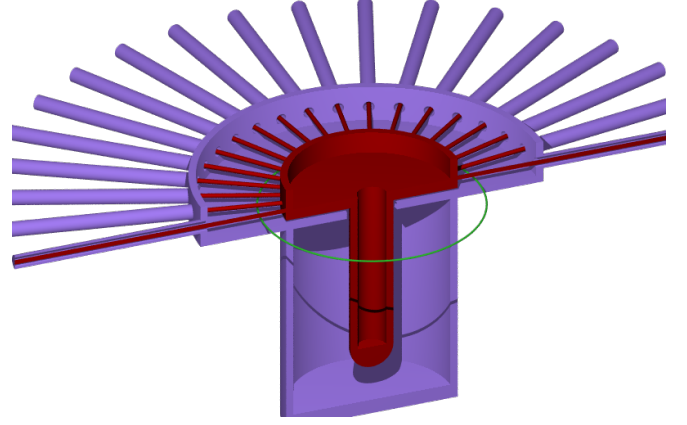


Fig. 4. Shown is a diagram of where the Faraday coil is placed on the Gemini DPF. In the cutaway, the red (darker) area represents the parts electrically connected to the anode, and the violet (lighter) areas are considered to be at cathode potential. The Faraday loop is shown as a hoop that is under the center center conductor wires, and above the ground plate.

to simulate resistive MHD in 2D and 3D high-deformation shocked media and pulsed power systems.

ALEGRA provides fine control over how the simulation is performed through a text file known as the "input deck." The primary purpose of the input deck is to define the simulation geometry, material composition, and physics to be modeled, though it also allows a user to request output and provide runtime controls. Part of defining the physics of a simulation is setting up the equations of state for the gases, which was among the most challenging aspects of the problem. Tabular equations of state provide the most effective means of modeling the thermodynamic state of material in the simulations, which may be in the solid, liquid, gaseous, or ionized state. Tabular EOS models were made available through ALEGRA's interface to Los Alamos National Laboratory's SESAME [14] data. Tabular representations of the Lee-More-Desjarlais (LMD) electrical and thermal conductivity model [15] were also used here. The LMD model combines empirical data with inferences from quantum molecular dynamics modeling and density functional theory (QMD-DFT) to provide a conductivity representation that spans the transition between conducting and insulating conditions and has proven quite successful in this "warm dense matter" regime [16], [17].

There are two approaches to defining the geometry on which to simulate the reaction using ALEGRA. The first is using ALEGRA's built-in functionality, by declaring pre-defined volumetric shapes (like spheres, prisms, pyramids, etc.) and defining the material composition of each shape. For example, many DPF machines have cylindrical copper cathode bars, and it is possible to define in the input deck a cylinder made of copper. The code then generates a 2D or 3D unstructured mesh that overlays the defined shapes, allowing for mesh elements to intersect more than one user-defined shape. The second approach to defining the geometry is by performing the computation on a body-fitted mesh generated

using an external meshing tool. The body-fitted mesh method is a more accurate method of describing the material in the simulation volume, but is more time-consuming to set up than the geometric method. ALEGRA's built-in functionality was used to define the geometry and material composition in all of the simulations shown in what follows, and boundary conditions are specified on subsets of nodes or faces within the simulation volume.

In any simulation, it is important that the geometry and the physics being simulated reflect the important geometries and physics of the experiment, and both raise several concerns in our simulations. For example, it is not necessary to include a faithful model of the vacuum chamber in our simulations, since the plasma does not interact with the top of the chamber during the simulation. Evaluating the physics being modeled, it is important to understand that the plasma in the DPF reaction is driven by an external electrical network, and a great strength of the ALEGRA-MHD code is that it has a sophisticated built-in circuit solver that can be used to couple electrical energy from user-specified circuits into the simulation volume.

Near the end of the simulation, just prior to the Z-pinch, the MHD simulation begins to become unphysical because of its inability to represent certain phenomena, such as, the kinetic instabilities which raise the plasma resistivity. The simulation may run past the point of Z-pinch without crashing, but the time-evolution of the simulation would be unphysical. Once the MHD simulation begins to approach the Z-pinch, it is possible to transfer the model state information to a particle-in-cell model to accurately simulate the Z-pinch, which has been demonstrated by researchers at LLNL[18] and SNL[8].

Setting up the initial condition for the simulation can also be tricky, since the DPF's starting state happens when the gas in the chamber breaks down in the vicinity of the insulating sheath and becomes a ring-shaped plasma shock. The breakdown of the gas is not covered by MHD physics, so the gas near the insulator has to be initialized in an artificial state that will quickly transition to the plasma shock known experimentally to exist in the DPF. We have found that setting up a thin layer of extremely hot ($\sim 10^6$ K, and therefore conductive) gas on the surface of the insulator results in the simulation initiating a plasma shock without causing observable artifacts in the time evolution of the simulation. Our experience with this initial condition is that the thin layer of hot gas should be about as thin as the Pyrex insulator and should touch both the anode and the cathode. Using this initiation of the plasma shock results in temperatures that match data from particle-in-cell calculations [8]. The artificially hot gas layer should stabilize its temperature near the shock temperature, $\sim 10^4$ K, within a few solver timesteps (typically, about 20 nanoseconds).

A. Two-dimensional Modeling

One and two dimensional models of the DPF are the most common in the literature, frequently coming in two generic types: empirical models and finite-element MHD models. The primary strength of empirical models, such as RADPFV5.5de [19], or Scat95 [20] is that they give results that are often very

close to experimental data. A significant drawback is that they require existing data to fit the model to, and can therefore only be used to simulate devices that are quite similar to the devices that one has experimental data for already. The second class are finite-element codes such as MHRDR [21] and Mach2 [22] that perform MHD modeling in one or two dimensions or in axis-symmetric 3D. Fully 3D MHD codes are not new, but can be hard to obtain and are usually more difficult to operate than 2D codes. Results of fully-3D DPF modeling are not well represented in the literature.

In many experimental realizations of the DPF, the cathode is a cylinder composed of metallic bars. While the plasma shock is traveling down the tube during rundown, the plasma spills outside of the anode-cathode gap through the spaces between the bars, a phenomenon that can be seen in the framing camera picture in Fig. 5. This can be approximated in 2D simulations, but in practice it is difficult to predict the time evolution of an actual DPF using these approximations.

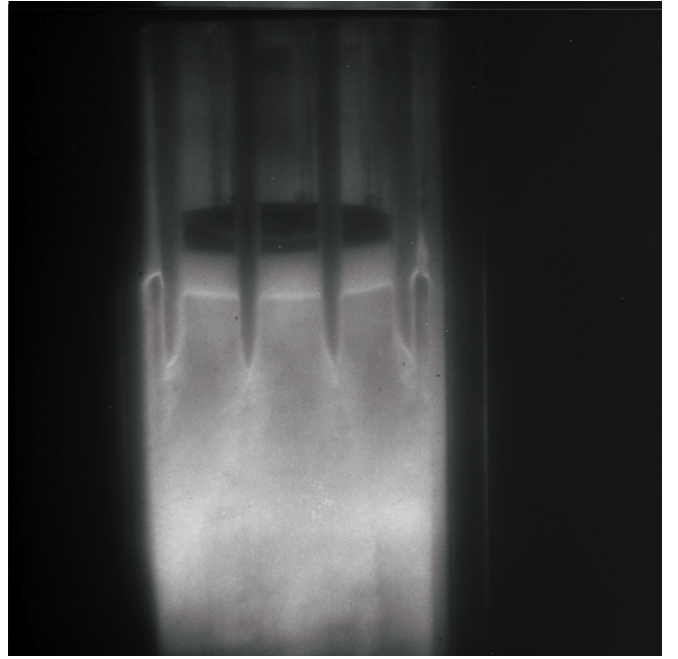


Fig. 5. Shown is a framing camera picture of the plasma rising up the electrodes in a DPF. The top of the anode can be seen as the dark disk in the middle of the bars, which can be seen at the top. The lower region of the chamber is bright due to the plasma, which has escaped the anode-cathode gap and surrounded the bars.

Simulations in 2D also impose other geometric constraints: the current density must either be completely in the radial-axial plane, or perpendicular to it, but not both at the same time. This precludes modeling situations that may have currents flowing helically, or situations in which the current may be flowing asymmetrically or off-axis. These restrictions on 2D simulations are often not of concern to investigators, who may want to ensure symmetry and simplicity in their experiments in order to simplify the data they collect. Nonetheless, the most general, physically realizable simulations are essential for complete understanding.

The 2D simulation that was run in ALEGRA made the

ad hoc assumption that there was a lower density floor below which the material was assumed to have no electrical or thermal conductivity. The floor was set at a density of $2.5 \times 10^{-4} \text{ kg/m}^3$, which was necessary in order to eliminate unphysical behavior in the simulation. The LMD model for deuterium plasma, shown in Figure 6, attributes moderate electrical conductivity to the plasma at this density for temperatures higher than approximately 1 eV, and this behavior is suppressed here, in order to cause the plasma shock to travel properly down the anode of the DPF.

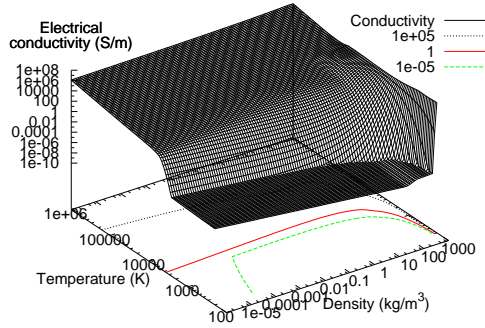


Fig. 6. The Lee-More-Desjarlais (LMD) electrical conductivity model for deuterium.

B. Three-dimensional Modeling

Fully 3D magnetohydrodynamic codes are available, such as ALEGRA and NIMROD [23], among others, and the benefit of using these codes is that the electrode geometry in the DPF can be modeled and simulated. The ability to investigate the effects of electrode structures without presupposing symmetries allows investigators to gain deeper understanding into how the plasma shock evolves over time. The primary drawback of 3D MHD modeling is the computational complexity of solving the MHD equations on large meshes, requiring computer clusters to perform simulations in a reasonable amount of time. Similar to the 2D modeling, the 3D modeling in ALEGRA required the imposition of a density floor at $2.5 \times 10^{-4} \text{ kg/m}^3$ in the electrical and thermal conductivity models.

Fig. 7 shows a representation of the material density midway through the rundown phase of the DPF in both the 2D and 3D simulations. The 2D modeling assumes axial symmetry, and the symmetry axis in both simulation volumes is on the far left-hand side. In the both simulations, the cathode bars are represented as rectangles on the right of the simulation domain, and the plasma shock travels from the bottom of the image to the top of the image, where it Z-pinches slightly above the hemispherical anode top. The plasma cannot flow

around the cathode bars in the 2D simulation as it can in the 3D simulation. The 3D simulation simulates the entire gas volume of the chamber, and it can be seen in Fig. 7 that the plasma is slightly slower and less dense in the 3D simulation than in the 2D simulation. The larger inductance results in longer rundown times and lower maximum current as compared to the 2D simulation, if all other system parameters are equal.

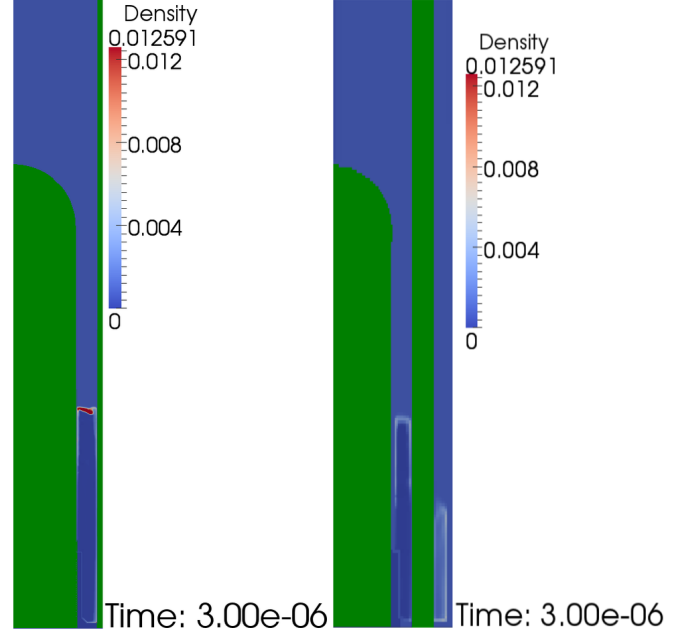


Fig. 7. This is a comparison of the density on a slice through the simulation volume at about 3 microseconds. The image on the left shows the 2D simulation where the plasma cannot flow around the bars, and the image on the right shows the 3D simulation, where the plasma can flow around the bars. Since the plasma flows around the bars in the 3D simulation, it also affects the external impedance as a function of time for the simulation volume.

IV. EXPERIMENTAL AND PREDICTED RESULTS COMPARISON

Fig. 8 shows the current profiles from a 3D simulation, two 2D simulations, and from the Faraday diagnostic of an actual experimental run. The “simulated current” in 2D (red, dashed line) and 3D (yellow, dash-dotted line) were both initiated using the same voltage and pressure as the experimental data. The 2D simulation predicts a peak current of 2.08 MA, which differs from the peak current measured by the Faraday diagnostic (2.17 MA) by only 4%. The 3D simulation systematically predicts lower peak currents, due to the higher inductance of the plasma escaping the cathode bars, and estimates peak current at 1.82 MA, an error of approximately 16%. Thus, for estimating peak current, the 2D simulation is more accurate than the corresponding 3D simulation.

The more important quantity of interest, however, is the duration time of the rundown phase of the reaction. The end of the rundown phase is defined at the point of maximum derivative of the current profile, which is $6.96 \mu\text{sec}$ for the experimental data. The 3D simulation predicts $6.69 \mu\text{sec}$, an

error of less than 4%, whereas the 2D simulation predicts a rundown time of $5.59 \mu\text{sec}$, an error of almost 20%, showing that the 3D simulation vastly outperforms the 2D simulation in predicting this quantity.

The two primary inputs into the ALEGRA simulation that we have discussed so far are the initial voltage and pressure, since these are the adjustable initial conditions of the DPF machine. The simulation allows for other quantities to be tweaked as well, though, and it is natural to adjust the model parameters to attempt to match the experimental data more closely. This is difficult with the 3D simulations, since they are too computationally intensive to “tweak” parameters one at a time and analyze the changes in output. For the 2D simulations, however, this is possible, and Fig. 8 shows the results of a 2D simulation (“tweaked current,” pink dotted line) that was designed to match the rundown time of the experimental results. This required that the series inductance be adjusted from 25 nH to 28.2 nH. Note that there is no experimental justification for this change, it is done just to show that the true rundown time can be achieved with a 2D simulation. This simulation does not outperform the 3D, however, since the 2D simulation matching the experimental rundown time results in a far inferior peak current measurement. Thus a small improvement in rundown time over the 3D gives a large degradation in peak current.

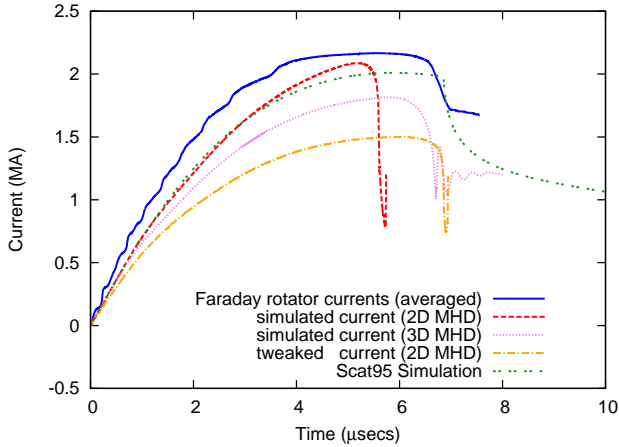


Fig. 8. Shown is a comparison of the simulated 2D current (red, dashed line) to the current measured by the Faraday probe (blue, solid line) and to the simulated 3D current (yellow, dash-dotted line) and a Scat95 simulation (green, dotted line). The 2D simulation underestimates peak current and severely underestimates rundown time. The 3D simulation also underestimates peak current but more faithfully predicts rundown time. Also shown is a 2D simulation (pink, dotted line) whose input parameters are adjusted to give a rundown time similar to the experimental data. In order that the 2D simulation match the experimental rundown time, the peak current is severely underestimated. The Scat95 simulation shows better agreement, however, requires iterative adjustment of parameters to already existing experimental data.

Naturally one should use simulation input parameters that represent the experiment being simulated as faithfully as possible, and the story of Fig. 8 is that 2D simulations of a DPF can give quite good results when the peak current is the quantity of interest. When the rundown time is of interest, which is more often the case, it is necessary to use

the fully 3D simulation to accurately predict the rundown time of an experiment. For comparison, a Scat95 simulation was iteratively adjusted to match the experimental data. While the agreement is good for this simulation, the parameters used in the match are only good matches for geometries and setups that are close to this particular case. Otherwise Scat95 achieves results that are similar to the 2D MHD simulations.

V. CONCLUSIONS

In this work we have presented results of fully 3D predictive simulations of a Dense Plasma Focus, using the ALEGRA MHD code from Sandia National Laboratories. As opposed to 2D or axis-symmetric 3D simulations, the fully 3D models more faithfully predict the duration of the rundown phase of the DPF, which is essential for ensuring that the maximum current runs through the system at the time of Z-pinch, which is required to accurately predict neutron yield. The 2D simulations are appropriate for predicting the peak current in the DPF, but are not capable of matching both the peak current and rundown time simultaneously.

ACKNOWLEDGMENT

The authors would like to thank Aaron Luttmann for helpful comments and suggestions on the manuscript. We would also like to thank Chris Hagen for providing support and encouragement for this project, as well as his insight into the theoretical and experimental operation of the DPF.

Sandia National Laboratories is a multi-program laboratory managed and operated by Sandia Corporation, a wholly owned subsidiary of Lockheed Martin Corporation, for the U.S. Department of Energy’s National Nuclear Security Administration under contract DE-AC04-94AL85000.

This manuscript has been authored in part by National Security Technologies, LLC, under Contract No. DE-AC52-06NA25946 with the U.S. Department of Energy and supported by the Site-Directed Research and Development Program. The United States Government retains and the publisher, by accepting the article for publication, acknowledges that the United States Government retains a non-exclusive, paid-up, irrevocable, world-wide license to publish or reproduce the published form of this manuscript, or allow others to do so, for United States Government purposes.

REFERENCES

- [1] J. W. Mather, “Investigation of the High Energy Acceleration Mode in the Coaxial Gun,” *Phys. Fluids. Suppl.*, vol. 7, S28, 1964.
- [2] J. W. Mather, “Formation of a High-Density Deuterium Plasma Focus,” *Phys. Fluids*, vol. 8, no. 2, Feb., 1965, pp. 366-377.
- [3] N. V. Filipov, T. I. Filipova, and V. P. Vinogradov, “Dense, High Temperature Plasma in a Noncylindrical Z-pinch Compression,” *Nuc. Fusion*, vol. 2, 577, 1962.
- [4] V. A. Gribkov, L. Mahe, P. Lee, S. Lee, A. Srivastava, “Dense Plasma Focus radiation source for microlithography & micro-machining,” *Proc. SPIE Microlithographic Techniques Integrated Circuit Fabrication II*, vol. 4226, 2000, pp. 151-159.
- [5] E. J. Lerner, S. K. Murali and A. Haboub, “Theory and Experimental Program for p-B11 Fusion with the Dense Plasma Focus,” *J. Fusion Energy*, vol. 30, no. 5, Jan., 2012, pp. 367-376.
- [6] J. O. Pouzo, “Applications of the dense plasma focus to nuclear fusion and plasma astrophysics,” *Plasma Science, IEEE Trans.*, vol. 31, no. 6, Dec., 2003, pp. 1237-1242.

- [7] J. H. Gonzalez, F. R. Brollo, and A. Clausse, "Modeling of the Dynamic Plasma Pinch in Plasma Focus Discharges Based in Von Karman Approximations," *Plasma Science, IEEE Transactions on*, vol. 37, no. 11, pp. 2178-2185, Nov., 2009.
- [8] C. S. Kueny, D. G. Flicker, and D. V. Rose, "ALEGRA-HEDP Simulations of the Dense Plasma Focus," Sandia National Laboratories, Albuquerque, NM, SAND2009-6373, 2009.
- [9] T. J. Murphy, "A practical Beryllium activation detector for measuring DD neutron yield from ICF targets," *LA-UR-96-1649* Los Alamos Unclassified Report, 1996.
- [10] B. T. Meehan, E. C. Hagen, C. L. Ruiz, G. W. Cooper, "Praseodymium activation detector for measuring bursts of 14 MeV neutrons," *Nucl. Instr. and Meth. A*, vol. 620, 2010, pp. 397-400.
- [11] O. Zucker, et al., "The plasma focus as a large fluence neutron source," *Nucl. Instrum. and Meth.*, vol. 145, issue 1, Aug., 1977, pp. 185-190.
- [12] W. J. Rider, A. C. Robinson, et al., "ALEGRA: An Arbitrary Lagrangian-Eulerian Multimaterial, Multiphysics Code," *Proc. 46th AIAA Aero. Sci. Meeting.*, Reno, NV, Jan., 2008.
- [13] L.R. Veaser, G.W. Day, "Fiber-Optic, Faraday Rotation Current Sensor," *LA-UR-86-2084* Los Alamos Unclassified Report, 1984.
- [14] S. P. Lyon, J. D. Johnson, "SESAME: The Los Alamos National Laboratory equation of state database," *LA-UR-92-3407* Los Alamos Unclassified Report, 1992.
- [15] M. P. Desjarlais, "Practical Improvements to the Lee-More Conductivity Near the Metal-Insulator Transition," *Contrib. Plasm. Phys.*, vol. 41, 2001, pp. 267-270.
- [16] M. K. Matzen, M. A. Sweeney, R. G. Adams, J. R. Asay, J. E. Bailey, et al., "Pulsed-power-driven high energy density physics and inertial confinement fusion research," *Phys. Plasmas*, vol. 12, no. 055503, 2005.
- [17] R. M. Lemke, M. D. Knudson, C. A. Hall, T. H. Haill, M. P. Desjarlais, J. R. Asay, "Characterization of magnetically accelerated flyer plates," *Phys. Plasmas*, vol. 10, no. 4, 2003, pp. 1092-1099.
- [18] A. Schmidt, V. Tang, D. Welch, "Fully Kinetic Simulations of Dense Plasma Focus Z-Pinch Devices," *Phys. Rev. Letters*, vol. 109, 205003 (2012).
- [19] S. Lee, S. H. Saw, et al., "Characterizing Plasma Focus Devices - Role of the Static Inductance - Instability Phase Fitted by Anomalous Resistances," *J. Fusion Energy*, vol. 30, no. 4, Aug. 2011pp. 277-282.
- [20] R. Gribble, M. Yapuncich, W. Deninger, "SCAT95," 2.0 Los Alamos National Laboratory, 1997.
- [21] V. Makhin, B. Bauer, et al., "Numerical Modeling of a Magnetic Flux Compression Experiment," *Journal of Fusion Energy*, vol. 26, 109-112, 2007.
- [22] M. H. Freese, "MACH2: A Two-Dimensional Magnetohydrodynamic Simulation Code for Complex Experimental Configurations," AMRC-R-874, (1987).
- [23] C. R. Sovinec, A. H. Glasser, et al., "Nonlinear Magnetohydrodynamics with High-order Finite Elements," *J. Comp. Phys.*, 195, 335 (2004).

B. T. Meehan received a B.S. in Physics from the United States Naval Academy in 1995 and an M.S. in Applied Physics from Stanford University in 1997. Currently he works with the Dense Plasma Focus Group at National Security Technologies, LLC, modeling DPFs with magnetohydrodynamics codes.

J. H. J. Niederhaus holds a B.S. in Physics from the Virginia Military Institute (2001), an M.S. in Nuclear Engineering from the Pennsylvania State University (2003), and a Ph.D. in Engineering Physics from the University of Wisconsin-Madison (2007). He is a computer scientist in the Computational Shock and Multiphysics Department at Sandia National Laboratories.